

Modeling planar pantographic sheets using a nonlinear Euler–Bernoulli beam element based on B-spline functions

Giuseppe Capobianco^{1,*}, Simon R. Eugster¹, and Tom Winandy¹

¹ Institute for Nonlinear Mechanics, University of Stuttgart, Stuttgart, Germany

An undeformed pantographic sheet consists of two orthogonal arrays of straight fibers interconnected by internal pins. In this paper, we model the fibers of this lattice-like sheet as nonlinear Euler–Bernoulli beams and use B-spline functions for their finite element discretization. Using the concept of one-dimensional generalized force laws, we show how different models for the pins can be introduced in the model. Finally, the simulation of a tensile test is presented.

Copyright line will be provided by the publisher

A pantographic sheet is a 3D printed structure which consists of two layers, each consisting of parallel fibers. These layers lie on top of each other and are orientated such that the fibers are orthogonal to each other. At every crossing point, the fibers of the upper and lower layers are interconnected by a pin, which gives the pantographic sheet a lattice-like structure. The rectangular pantographic sheet is clamped to a block at both ends, see Fig. 3. To describe the deformation of a pantographic sheet, we model each beam as a planar, nonlinear Euler–Bernoulli beam which we discretize using the finite element approach with B-spline shape functions. To model the pins and the clamping, we introduce one-dimensional generalized force laws with suitable constitutive relations. Our approach is similar to the one used in [1]. For more details on the modeling of pantographic sheets and some experimental validation of these models, we refer to [1, 2].

The Euler–Bernoulli assumption, demanding the cross sections of the beam to remain orthogonal with respect to its centerline, allows to formulate the kinematics of the i -th beam using the deformation of the centerline only. We parametrize the centerline of the i -th beam of length L_i by a parameter $\xi \in [0, 1]$ and describe the position of a point on the centerline in the reference configuration by $\mathbf{X}_i(\xi) = X_i(\xi)\mathbf{e}_x + Y_i(\xi)\mathbf{e}_y$ and in the deformed configuration by $\mathbf{x}_i(\xi) = x_i(\xi)\mathbf{e}_x + y_i(\xi)\mathbf{e}_y$, cf. Fig. 1. Denoting with prime the derivative with respect to ξ , we introduce the tangent vectors $\mathbf{G}_i = \mathbf{X}'_i$ and $\mathbf{g}_i = \mathbf{x}'_i$ to the centerline. Their inclinations are described by the angles Φ_i and φ_i , respectively. Denoting the lengths of the tangent vectors

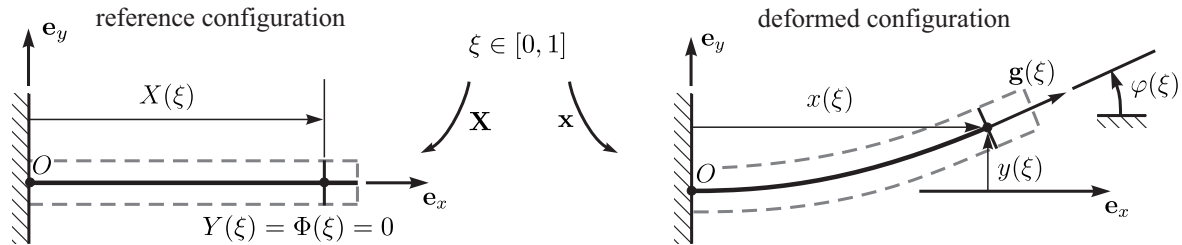


Fig. 1: Kinematics of the Euler–Bernoulli beam. Index i is omitted.

measured in the Euclidean norm as $G_i = \|\mathbf{G}_i\|$ and $g_i = \|\mathbf{g}_i\|$, we introduce as deformation measures of the beam the axial stretch λ_i and the material curvature κ_i as

$$\lambda_i(\xi) = \frac{g_i(\xi)}{G_i(\xi)} \quad \text{and} \quad \kappa_i(\xi) = \frac{\varphi'_i(\xi)}{G_i(\xi)}. \quad (1)$$

We assume that the reference configuration is of the form $\mathbf{X}_i(\xi) = \xi L_i \mathbf{e}_x$, which leads to $G_i = L_i$ and $\Phi_i = 0$. Using the variations $\delta\lambda_i$ and $\delta\kappa_i$ of the deformation measures (1) and assuming linear elastic constitutive laws for the axial force N_i and the bending moment M_i , the internal virtual work of the i -th beam is given by

$$\delta W_i^{\text{int}} = - \int_0^1 \{N_i(\xi) \delta\lambda_i(\xi) + M_i(\xi) \delta\kappa_i(\xi)\} G_i d\xi, \quad \text{with } N_i = EA_i(\lambda_i - 1) \text{ and } M_i = EI_i \kappa_i, \quad (2)$$

where EA_i and EI_i are the axial and the bending stiffnesses of the beam. For a Galerkin-type finite element discretization of the beam, we approximate its centerline by B-spline polynomials. This approximation can be written in the form $\mathbf{x}_i(\xi) = \mathbf{N}_i(\xi) \mathbf{q}_i$, where \mathbf{N}_i is the matrix of B-spline basis functions and \mathbf{q}_i is the vector consisting of the coordinates of the control points, cf. [3]. Computing the stretch measures $\lambda_i(\xi, \mathbf{q}_i)$ and $\kappa_i(\xi, \mathbf{q}_i)$, using the approximation in (1) and assuming that their variations used in (2) are induced by a virtual displacement $\delta \mathbf{q}_i$ of the control points, the discretized internal virtual work is

$$\delta W_i^{\text{int}} = - \int_0^1 \left\{ N_i(\xi, \mathbf{q}_i) \frac{\partial \lambda_i}{\partial \mathbf{q}_i} + M_i(\xi, \mathbf{q}_i) \frac{\partial \kappa_i}{\partial \mathbf{q}_i} \right\} \delta \mathbf{q}_i G_i d\xi = \mathbf{f}_i^{\text{int}}(\mathbf{q}_i)^T \delta \mathbf{q}_i, \quad (3)$$

* Corresponding author: capobianco@inm.uni-stuttgart.de

where we have introduced the discrete internal force vector $\mathbf{f}_i^{\text{int}}$ of the i -th beam. We model every fiber segment connecting two pins of the pantographic sheet as such a discretized Euler–Bernoulli beam, see Fig. 2. Assuming that the pantographic sheet is modeled by n_b beams, the degrees of freedom of the pantographic sheet are the collection $\mathbf{q} = (\mathbf{q}_1^T \dots \mathbf{q}_{n_b}^T)^T$ of all control point coordinates.

To model the pins and the clamping, we introduce one-dimensional generalized force elements. The kinematics of such a force element is described by a scalar function g , called gap function. The force f of the force element exerted on the pantographic sheet can be modeled by a constitutive force law relating f to g . According to [4], the virtual work contribution of a one-dimensional force law is given by the product of the variation of the gap and the force, i.e.

$$\delta W^{\text{fl}} = \delta g f = \delta \mathbf{q}^T \left(\frac{\partial g}{\partial \mathbf{q}} \right)^T f. \quad (4)$$

We model the pin between the discretized Euler–Bernoulli beams i, j, k and l using several force elements, cf. Fig. 2. First the end points of the beams k and j are joined by the two ideal constraint force laws $-f_{1/2}^c \in \mathbb{R}$ s.t. $g_{1/2}^c(\mathbf{q}) = 0$ with $g_1^c(\mathbf{q}) = \mathbf{e}_x \cdot (\mathbf{x}_k(1) - \mathbf{x}_j(0))$ and $g_2^c(\mathbf{q}) = \mathbf{e}_y \cdot (\mathbf{x}_k(1) - \mathbf{x}_j(0))$. The same is done for the beam pairs (i, l) and (i, j) . To account for the fact that the beams i and l are of the same fiber of the pantographic sheet, the ideal constraint force law $-f_3^c \in \mathbb{R}$ s.t. $g_3^c(\mathbf{q}) = 0$ with $g_3^c(\mathbf{q}) = \varphi_i(1) - \varphi_l(0)$ is introduced to achieve that the two beams have the same tangent orientation at their connection point. The same is done for the beam pair (j, k) . These constraints together result in an ideal pivot between the fibers. The torsional stiffness of the pin is modeled by adding a linear torsional spring with stiffness c described by the force law $-f_1^s(\mathbf{q}) = c g_1^s(\mathbf{q})$ with $g_1^s(\mathbf{q}) = \varphi_i(1) - \varphi_j(0) + \pi/2$. In an analogous manner, we can model the clamping of the pantographic sheet to the environment by additional ideal constraint force laws.

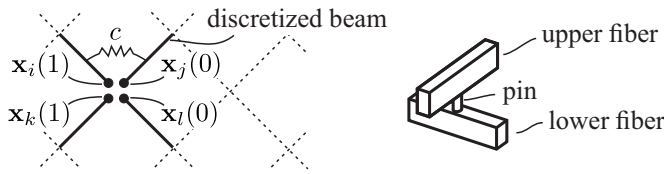


Fig. 2: Modeling of a pin (left) illustration of a real pin (right).

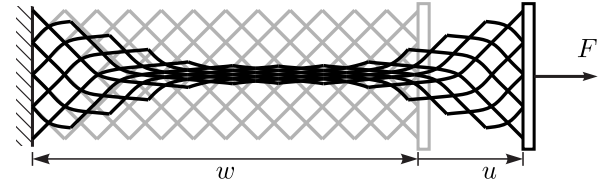


Fig. 3: Simulation of a tensile test. Undeformed (gray) and deformed (black) configuration.

Summing up all the virtual work contributions modeling the pantographic sheet, the total virtual work is

$$\delta W^{\text{tot}} = \delta \mathbf{q}^T \left[\sum_{b=1}^{n_b} \mathbf{f}_b^{\text{int}}(\mathbf{q}) + \sum_{i=1}^{n_s} \left(\frac{\partial g_i^s}{\partial \mathbf{q}} \right)^T f_i^s(\mathbf{q}) + \mathbf{f}^{\text{ext}}(\mathbf{q}) + \sum_{j=1}^{n_c} \left(\frac{\partial g_j^c}{\partial \mathbf{q}} \right)^T f_j^c \right], \quad (5)$$

where with \mathbf{f}^{ext} we have accounted for external forces acting on the pantographic sheet and n_s and n_c denote the number of springs and ideal constraints, respectively.

By the principle of virtual work, the total virtual work (5) of the pantographic sheet has to vanish for all virtual displacements $\delta \mathbf{q}$, which implies that the expression in square brackets has to be equal to zero. This together with the constraint equations $g_j^c(\mathbf{q}) = 0$ for $j = 1, \dots, n_c$ results in a system of nonlinear algebraic equations for the control point coordinates \mathbf{q} of the B-spline shape functions and for the constraint forces f_j^c . This system of equations is solved using the Newton–Raphson method.

Fig. 3 shows the simulation result of a tensile test. The simulated pantographic sheet has an undeformed width of $w = 0.21[\text{m}]$. The stiffnesses $EA_i = 2304[\text{N}]$, $EI_i = 1.555 \cdot 10^{-4}[\text{Nm}^2]$ and $c = 0.004[\text{N}]$ have been assumed. Fifth order B-spline polynomials with one element per beam have been used for the simulation and the integral in (3) has been approximated by a Gaussian quadrature with five points per element. For an external force $F = 10.29[\text{N}]$ an elongation $u = 0.048[\text{m}]$ has been computed.

The modeling approach used in this paper is very versatile. Using the concept of ideal constraint force laws, we can implement different boundary conditions and other models of the pin can be realized by combining different one-dimensional force laws. For instance, we can account for a finite shear stiffness of a pin by replacing the ideal force laws introduced between the pair of beams (i, j) with a linear spring with stiffness k characterized by the force law $-f_2^s(\mathbf{q}) = k g_2^s(\mathbf{q})$ with $g_2^s(\mathbf{q}) = \|\mathbf{x}_i(1) - \mathbf{x}_j(0)\|$. Obviously also nonlinear constitutive equations for the spring are allowed and can be treated in the same way.

References

- [1] U. Andreaus, M. Spagnuolo, T. Lekszycki, and S. R. Eugster, Continuum Mech. Therm. pp. 1–21 (2018).
- [2] L. Placidi, E. Barchiesi, E. Turco, and N. L. Rizzi, Z. Angew. Math. Phys. **67**(5), 121 (2016).
- [3] L. Piegl and W. Tiller, The NURBS Book (Springer, 1997).
- [4] C. Glocker, Set-Valued Force Laws: Dynamics of Non-Smooth Systems, (Springer, 2001).